Active LQR and $\mathcal{H}_2$ shunt control of electromagnetic transducers.

Andrew J. Fleming, Sam Behrens and S. O. Reza Moheimani
The School of Electrical Engineering and Computer Science
University of Newcastle, Callaghan 2308, Australia
andrew@ee.newcastle.edu.au

***Abstract*— Electromagnetic transducers have been used extensively for active feedback control of mechanical vibration. In this paper, we demonstrate a new technique where an electrical impedance, connected to the terminals of an electromagnetic actuator, is designed to reduce vibration in the host structure. By measuring the coil terminal voltage and controlling the resultant current or *vice-versa* the coupled mechanical system can be controlled. The problem is cast as a standard MIMO control objective to facilitate automatic design of the electrical impedance by such means as regular LQR or $\mathcal{H}_2$ controller synthesis. Potential applications include: vehicle suspension systems, vibration isolation platforms, and the control of enclosed-sound fields. Active impedance controllers require no external sensors. The presented techniques are verified experimentally through the application to a single-degree-of-freedom system.**

I. Introduction

Electromagnetic transducers [9], [11], [7] can be used as actuators, sensors, or both. When a current is applied to the terminals of an electromagnetic transducer, a force is exerted, conversely, when a transducer experiences a velocity, an open-circuit voltage is induced. Piezoelectric transducers [6], exhibit similar electromechanical properties but are characterized by a high mechanical impedance. Electromagnetic transducers are capable of significantly greater strokes, typically in the millimeter range compared to the micrometer range.

In analogy to the technique of piezoelectric self-sensing [4], [1], a recent literature has also developed on the topic of electromagnetic self-sensing actuators [12], [2], [10], [7], [8]. This technique involves estimating the system velocity from the measured coil current whilst applying a driving voltage to the transducer. An example of this technique can be found in [3], where the acoustic preasure of an enclosed-sound field is estimated from the measured current flowing through an actuating speaker coil. A feedback loop, driving the speaker voltage, is constructed around the estimate to minimize the acoustic response of the enclosure.

In this paper, we demonstrate the modelling, design, and implementation of active impedance controllers for electromagnetically actuated systems. By measuring the coil terminal current and controlling the resultant voltage, effectively implementing some electrical impedance, it is possible to obtain control over the mechanical system. After revealing the underlying feedback structure and casting it as a standard MIMO control problem, the application of synthesis techniques such as LQR and $\mathcal{H}_2$ is straight-forward.

Although, the focus is on the control of a system similar to an isolation column, the generality of the modelling and design framework is intended to be extensible to a large class of mechanical systems. Such applications include: MIMO vehicle suspension systems, vibration isolation platforms, and the control of enclosed-sound fields. Active admittance or impedance controllers require no external sensors, are capable of minimizing a pre-specified peformance objective, and can also be used to esitmate physical variables dynamically related to the system states such as velocity.

Experimentally, the presented techniques are verified through their application to a single-degree-of-freedom mechanical system.

This paper is presented in 5 sections. In Section 2, we begin with the modelling of mechanical, electromagnetic, and composite systems. We then present a method in Section 3 for the design of active impedance controllers to minimize a time domain (LQR) and frequency domain ($\mathcal{H}_2$) preformance objective. The presented techniques are then applied to an experimental electromagnetic system in Section 4. Finally, the paper is concluded in Section 5.

II. Modelling

This section introduces a modelling technique for the design and analysis of shunted electromechanical systems. Although the focus is on a single-degree-of-freedom system, the process is quite general and can easily be extended to more complex mechanical systems.

A. Electromagnetic System

When an electrical conductor, in the form of a coil, moves in a magnetic field a voltage V proportional to the velocity $\dot{x}$ is induced and appears across the terminals of the coil. Specifically,

$$\frac{V}{\dot{x}} = Bl, \tag{1}$$

where B is the magnetic flux (in Teslas), l is the length of the conductor (in meters), and $\dot{x}$ is the velocity of the conductor relative to the magnetic field (in ms^{-1}). A permanent magnet is usually the source of the magnetic field. In another configuration the coil is kept stationary and the magnet is made to move.

Assuming the coil is exposed to a field of constant flux density and the relative displacement is small, Equation (1) can be rewritten [11] as,

$$\frac{V}{\dot{x}} = \frac{F}{I} = Bl = C_n, \tag{2}$$

where F denotes the force (in Newtons) acting on the coil carrying a current I (Amps), and C_n is the ideal electromechanical coupling coefficient.

When the coil is employed as a force actuator, Equation (2) relates the induced force to an applied current. Electrodynamic shakers and acoustic speakers operate on this principle.

An electromagnetic coil can be modeled as the series connection of an inductor L, a resistor R, and a dependent voltage source V [7]. When coupled to a mechanical system, the induced emf and hence mechanical velocity can be determined from the open-circuit coil terminal voltage.

B. Mechanical System

The input/ouput model of a general mechanical system is shown in Figure 2 (a), the mechanical plant is denoted P. In addition to various application specific inputs and outputs, to couple the system to an electromagnetic actuator, the model requires a force input F_e and a velocity output $\dot{x}$. In a typical sceanario, the model would also descibe the influence of a specific disturbance input w.

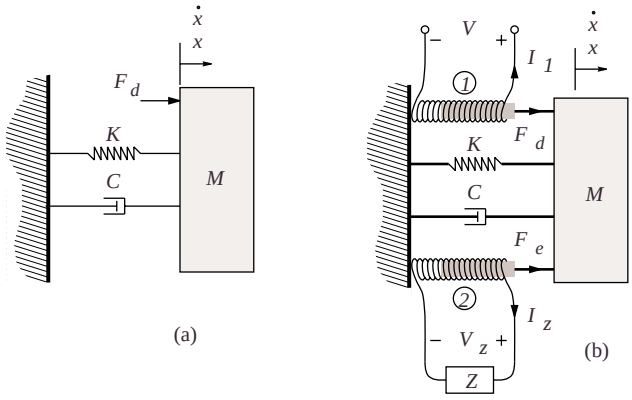

Fig. 1. Mass-spring-damper system (a), coupled to two electromagnetic coils (b).

In many cases where vibration becomes an issue, the mechanical structure can be modeled as the simple mass-spring-damper system shown in Figure 1 (a). Examples include, but are not limited to: isolation columns, magnetic bearings, and suspension systems.

The equation of motion for a forced one degree of freedom system is,

$$M\ddot{x}(t) + C\dot{x}(t) + Kx(t) = F_d(t), \tag{3}$$

where $F_d(t)$ is the applied force, M is the equivalent mass (in kg), K is the spring constant (in N/m), C is the damping constant (in Ns/m), and $\ddot{x}(t)$, $\dot{x}(t)$ and $x(t)$ are the acceleration, velocity and displacement respectively. In the Laplace domain, the transfer function $G_{\dot{x}F}(s)$ from an applied force to the resulting velocity is,

$$G_{\dot{x}F}(s) = \frac{s\,x(s)}{F_d(s)} = \frac{\frac{1}{M}}{s^2 + s\frac{C}{M} + \frac{K}{M}}. \tag{4}$$

In later sections we will also require the following minimal state-space model for $G_{\dot{x}F}(s)$,

$$\begin{aligned} \dot{x}_p(t) &= \mathbf{A}_p x_p(t) + \mathbf{B}_p F_e(t) \\ \dot{x}(t) &= \mathbf{C}_p x_p(t) \end{aligned} \tag{5}$$

Consider Figure 1 (b), where a single-degree-of-freedom system is coupled to two electromagnetic coils. Coil 1 is used to introduce a force disturbance and coil 2 to control the resulting vibration. The corresponding mechanical plant model P is shown in Figure 2 (a). The general constants C_1 through C_4 represent the various electromachanical coupling contants as defined in (6). The constants are defined individually as the two coils will neither be perfectly matched nor have exactly identical force-current or velocity-voltage ratios.

$$C_1 = \frac{F}{I_1} \quad C_2 = \frac{V_{e_1}}{\dot{x}} \quad C_3 = \frac{F}{I_2} \quad C_4 = \frac{V_{e_2}}{\dot{x}} \tag{6}$$

Using the constants defined in (6), the electromagnetic system E associated with coil 2 is shown in Figure 2 (b).

C. Shunted composite electromechanical system

We now consider a mechanical system $G_{\dot{x}F}(s)$ coupled to a shunted electromagnetic transducer as shown in Figure 1 (b). In this case, coil 1 is used to introduce a force disturbance F_d, and coil 2, the shunted coil, is used to control the resulting vibration.

Within the modeling framework introduced in the previous two subsections, it is a simple and intuitive task to construct the composite system. The interconnection of the electromagnetic system E and the mechanical plant model P is shown in Figure 2 (a).

In Figure 2 (a) the impedance $Z(s)$, interpreted simply as the transfer function relating the coil terminal current to voltage, appears like a feedback controller for the electromechanical system. By concatenating the mechanical and electromagnetic systems, P and E, as shown in Figure 2 (b), the composite system is cast as a typical regulation problem for the abstracted system G. It is easily shown that the closed-loop transfer function from an applied disturbance current $I_1(s)$ to the resulting plunger velocity $s\,x(s)$ is,

$$\frac{s\,x(s)}{I_1(s)} = \frac{G_{\dot{x}F}(s)C_1C_4}{1 + K(s)C_3C_4G_{\dot{x}F}(s)}, \tag{7}$$

where $K(s)$, the equivalent feedback controller is,

$$K(s) = \frac{1}{Ls + R + Z(s)}. \tag{8}$$

III. Control Design

As shown in Figure 2, and in Equation 7, the impedance connected to a mechanically coupled electromagnetic transducer can be viewed as parameterizing a feedback controller for the mechanical system $G_{\dot{x}F}(s)$. The following subsection introduces two techniques for the synthesis of active impedance and admittance controllers designed to minimize structural vibration.

A. Impedance synthesis

Referring to Figure 2, the shunted electromechanical system can be regarded as a typical control design problem where a disturbance I_1 results in a vibration characterized by the velocity $x(t)$.

In order to apply standard synthesis techniques such as LQR, we require a minimal state space model respresenting the composite system. By defining the following state-space model for the coil admittance $\frac{1}{Ls+R}$,

$$\begin{aligned} \dot{x}_y(t) &= \mathbf{A}_y x_y(t) + \mathbf{B}_y V(t) \\ I_z(t) &= \mathbf{C}_y x_y(t) \end{aligned} \tag{9}$$

where, for example, $\mathbf{A}_y = \left[-\frac{R}{L}\right]$, $\mathbf{B}_y = [1]$, and $\mathbf{C}_y = \left[\frac{1}{L}\right]$, a state-space model is easily derived for the composite system G.

$$\begin{aligned} \dot{x}_g(t) &= \mathbf{A}_g x_g(t) + \mathbf{B}_g \begin{bmatrix} I_1(t) \\ V_z(t) \end{bmatrix} \\ \begin{bmatrix} \dot{x}(t) \\ I_z(t) \end{bmatrix} &= \mathbf{C}_g x_g(t) \end{aligned} \tag{10}$$

where,

$$x_g(t) = \begin{bmatrix} x_p(t) \\ x_y(t) \end{bmatrix}, \; \mathbf{B}_g = \begin{bmatrix} \mathbf{B}_p C_1 C_4 & \mathbf{0} \\ \mathbf{0} & -\mathbf{B}_y \end{bmatrix}, \tag{11}$$

and

$$\mathbf{A}_g = \begin{bmatrix} \mathbf{A}_p & \mathbf{B}_p\mathbf{C}_y C_3 C_4 \\ \mathbf{B}_y\mathbf{C}_p & \mathbf{A}_y \end{bmatrix}, \; \mathbf{C}_g = \begin{bmatrix} \frac{1}{C_4}\mathbf{C}_p & \mathbf{0} \\ \mathbf{0} & \mathbf{C}_y \end{bmatrix}. \tag{12}$$

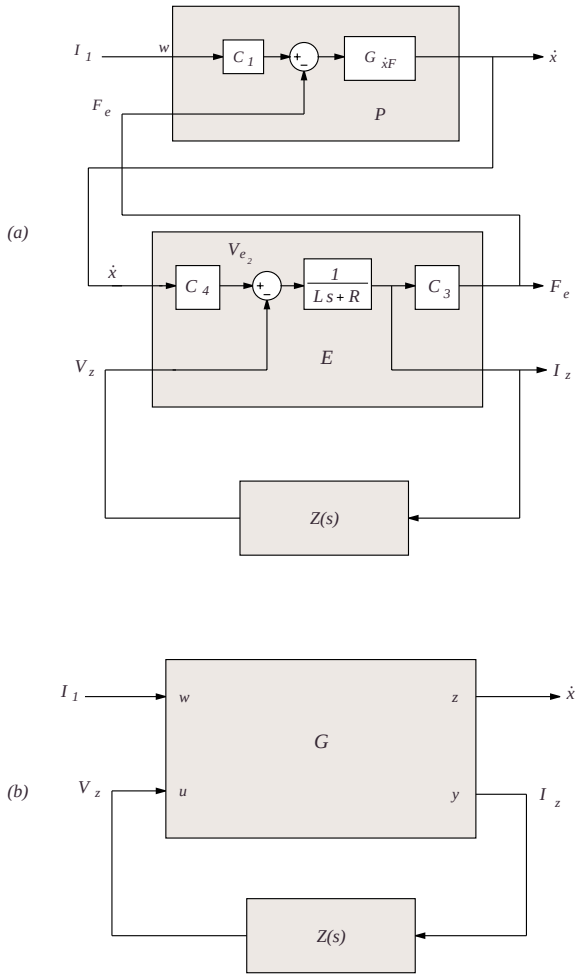

Fig. 2. The shunt admittance controlled electromechanical system (a), in generalized plant/controller form (b).

Our design objective is to minimize the velocity $\dot{x}(t)$ whilst restraining the magnitude of the control signal V_z. In a linear quadratic sense, the objective is to minimize,

$$J = \int_{-\infty}^{\infty} \dot{x}^2(t) + k_u V_z^2(t)\ dt \tag{13}$$

where k_u is the weighting on the control signal V_z. Restated, in the standard LQR context,

$$J = \int_{-\infty}^{\infty} x^{'}(t) Q x(t) + u^{'}(t) R u(t)\ dt, \tag{14}$$

the corresponding Q and R matrices are $Q = \left[\begin{array}{cc} \frac{1}{C_4}\mathbf{C}_p & \mathbf{0} \end{array} \right]^{'} \left[\begin{array}{cc} \frac{1}{C_4}\mathbf{C}_p & \mathbf{0} \end{array} \right]$, and $R = k_u$.

We can also consider the $\mathcal{H}_2$ control objective where we seek to minimize, in the $\mathcal{H}_2$ sense, the weighed sum of the velocity and control signal in response to a specific disturbance I_1, i.e., we seek to minimize,

$$J = \left\| \frac{s\ x(s) + k_u V_z(s)}{I_1(s)} \right\|_2 \tag{15}$$

Parameter	Value
Spring constant K	$56\ kNm^{-1}$
Damping coefficient C	$2.667\ Nsm^{-1}$
Plunger mass M	$0.150\ kg$
Electromagnetic Coupling C_1	3.55
Electromagnetic Coupling C_2	4.06
Electromagnetic Coupling C_3	3.55
Electromagnetic Coupling C_4	4.06
Coil Inductance L	$1\ mH$
Coil Resistance R	$3.3\ \Omega$

TABLE I
ELECTROMECHANICAL SYSTEM PARAMETERS.

This specification is easily cast as a standard $\mathcal{H}_2$ problem by considering the modified plant $\tilde{G}$ that includes a performance weighting on the control signal. Minimizing (15) is now equivalent to minimizing,

$$J = \left\| \frac{z(s)}{w(s)} \right\|_2 \tag{16}$$

where the modified plant $\tilde{G}$ is that of (10) with a non-zero D matrix,

$$\tilde{\mathbf{D}}_g = \left[\begin{array}{cc} \mathbf{0} & k_u \\ \mathbf{0} & \mathbf{0} \end{array} \right] \tag{17}$$

IV. EXPERIMENTAL RESULTS

To verify the modelling and design techniques presented in the preceding sections, each method was applied to an experimental electromechanical system.

A. *Electromagnetic Transducer*

A photograph of the electromagnetic transducer showing the rigid body, flexible end supports, mounting plate, and coils is provided in Figure 3. The apparatus is essentially a translational solenoid with two identical fixed coils and magnetic plunger supported at either end by flexible disks. A side section including dimensions and magnetic orientations is shown in Figure 4.

The coils are wound from $0.25\ mm$ diameter enamel coated copper wire and have an electrical impedance of $3.3\ \Omega$ + $1\ mH$. In order to prevent distortion of the magnetic flux field, only non-magnetic materials, such as aluminum and copper, were used in the construction of the rigid body, flexible end supports and mounting plate.

In practice, the magnetic field strength, as well as being a function of the magnetic material, is limited by the maximum allowable dimensions and weight of the magnets. In these experiments, three rare earth magnets (Neodymium Iron Boron), are arranged to form the magnetic plunger as shown in Figure 4. At the two points where opposing poles meet (at the center of each winding), a strong magnetic field exits at right angles to the plunger. When the plunger is in motion, the strong parallel field flowing through the coil results in a high flux density and correspondingly large induced voltage. The physical parameters of the electromagnetic and mechanical systems are summarized in Table I.

The plunger velocity is measured using a PSV-300 Polytec Scanning Laser Vibrometer.

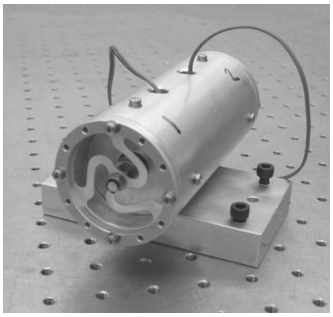

Fig. 3. An external photograph of the experimental electromagnetic apparatus.

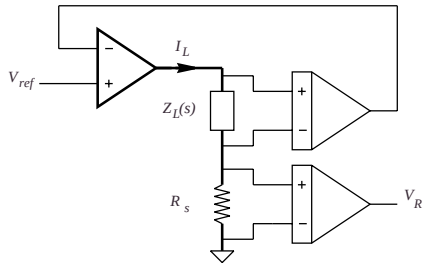

Fig. 5. The simplified schematic of a differential voltage feedback amplifier. The desired transducer voltage V_z is applied to the reference V_{ref}. The transducer is represented by the load impedance $Z_L(s)$. The sensing resistor R_s yields a measurement of the transducer current I_z which is proportional to the resistor voltage V_r.

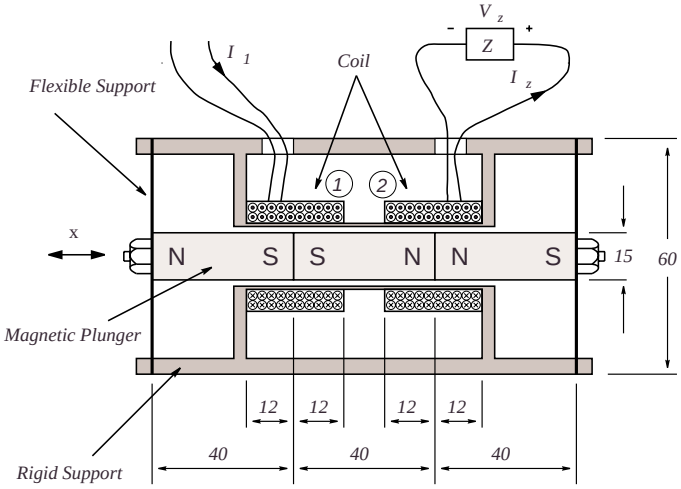

Fig. 4. Side section of the experimental electromagnetic apparatus.

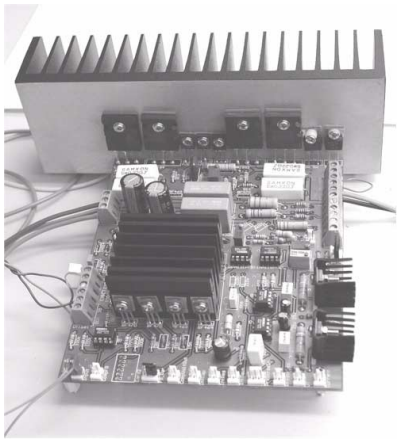

Fig. 6. Implementation of a voltage and current fluxion amplifier.

B. Power amplifier and instrumentation

In order to implement the arbitrary shunt impedances resulting from the control design, a power amplifier was developed capable of driving differential terminal voltages. The device is also capable of instrumenting the resulting load current.

The simplified schematic of such a circuit is shown in Figure 5. Within the high frequency bandwidth of the control loop, the reference potential V_{ref} appears accross the load, i.e. we have a unity gain voltage amplifier. The additional resistance and differential amplifer generate the current measurement V_R with gain R_s V/A.

A practical implementation of amplifier is shown in Figure 6. The device is capable of $\pm$ 200 V operation at a maximum DC current of 32 Amps. Further analysis and a more detailed discussion of the implementation can be found in [5].

A dSpace 1005 based system is used to implement the required impedance transfer functions.

C. Impedance synthesis

Figure 7 shows the instrumentation and driver gains associated with the underlying electromechanical system. The voltages V_1 through V_4 represent the signals applied to, or measured from, the power amplifiers and instrumentation. The gain and units associated with each signal can be found in Table II. The actual electrical shunt impedance presented to the coil is related to the controller through the gains k_3 and k_4, specifically,

$$Z_c(s) = \frac{V_z(s)}{I_z(s)} = k_3 C(s) k_4 \tag{18}$$

To assess the accuracy of the analytic model (discussed in Section II-C), the simulated frequency response is compared to that measured directly from the experimental system. A multivariable frequency response is measured successively from each input to output pair. During the component SISO

Gain	Value
k_1	1 A/V
k_2	40 V/ms^{-1}
k_3	-4 V/V
k_4	10 V/A

TABLE II

EXTERNAL GAINS ASSOCIATED WITH THE SHUNT VOLTAGE CONTROLLED ELECTROMAGNETIC SYSTEM

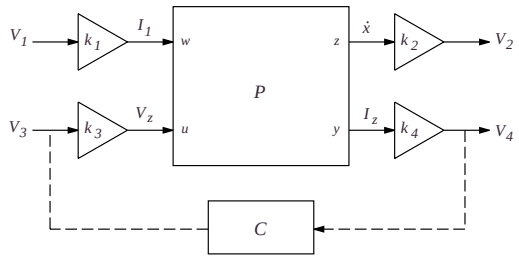

Fig. 7. Open-loop external gains of the shunt voltage controlled electromagnetic system.

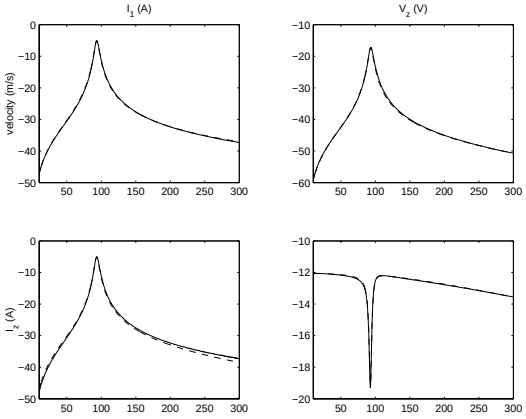

Fig. 8. The simulated (—), and experimental (- -), magnitude frequency response of the shunt voltage controlled electromagnetic system.

frequency response measurements, the residual input is set to zero. The magnitude and phase frequency responses are shown respectively in Figures 8 and 9. In the frequency domain, a good correlation can be observed between the analytic model and measured system.

1) LQR impedance synthesis: As discussed in Section III-A, a linear quadratic regulator can be designed to command the shunt terminal voltage V_z with a view to regulating a performance signal consisting of the weighted sum of plunger velocity and the control signal. An observer is required to estimate the system states from the measured shunt current I_z. Once designed, the concatenation of the observer and LQR gain matrix results in a system, interpreted as an active shunt impedance, that can be applied to one of the electromagnetic coils in order to reduce structural vibration.

Based on the physical model (including external gains) that was validated in the previous sub-section, and referring to the notation introduced in Section III-A, an LQR gain matrix was designed to minimize the following performance function,

$$J = \int_{-\infty}^{\infty} k_2 \dot{x}(t) + \frac{7}{k_3} V_z(t)\ dt, \tag{19}$$

where the factor 7 represents the relative control weighting. The gains k_2 and k_3 are included as the design is based on the input-output model which includes the amplifier and instrumentation dynamics. The observer was designed by pole placement, where the target poles were chosen as that of the closed-loop system with real components multiplied by 2. As is routine in control system design, the control

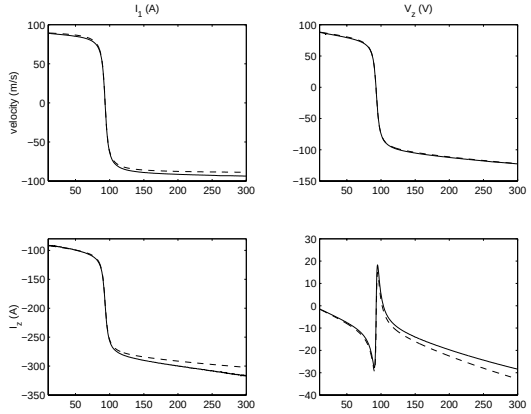

Fig. 9. The simulated (—), and experimental (- -), phase frequency response of the shunt voltage controlled electromagnetic system.

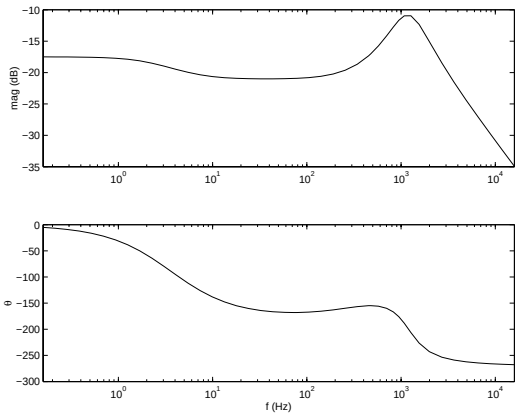

Fig. 10. Magnitude and phase response of the LQR impedance controller.

weighting of 7 and observer pole locations were chosen experimentally to achieve a reasonable trade-off between damping performance, robustness, and the control signal magnitude.

The frequency response of the positive feedback regulator is shown in Figure 10. The damping performance of the LQR controller was assessed in both the frequency and time domains. With the controller in the loop, a disturbance current I_1, proportional to a force disturbance, is applied to the system. Experimental and simulated open- and closed-loop frequency responses are shown in Figure 11. The controller was measured to reduce the resonant peak by 19.4 dB. The corresponding time domain velocity response to a 300 Hz low-pass filtered step change in disturbance current I_1 is shown in Figure 12. The simulated closed-loop step response was obtained by recording the applied step signal and applying it in simulation to the closed-loop model.

2) $\mathcal{H}_2$ impedance synthesis: In analogy to Section IV-C.1, and as discussed in Section IV-C.2, a shunt impedance was designed to minimize the $\mathcal{H}_2$ norm of the transfer function between a disturbance current I_1 and a performance signal z. As in Section IV-C.1, the performance signal consists of the weighted sum of plunger velocity and control signal.

For the plant under consideration, the $\mathcal{H}_2$ problem is well defined and feasible. All of the standard requirements

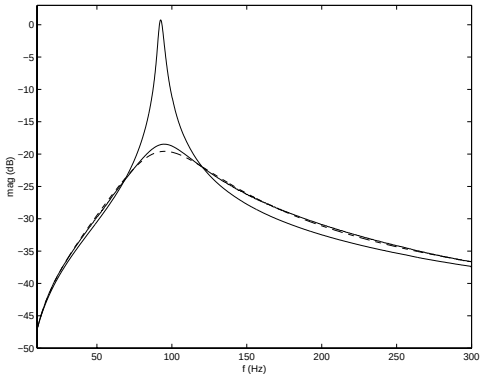

Fig. 11. The experimental (—) and simulated (- -), open- and closed-loop frequency responses from an applied disturbance current I_1 (A) to the resulting plunger velocity $\dot{x}$ (ms^{-1}) for the LQ impedance controlled system.

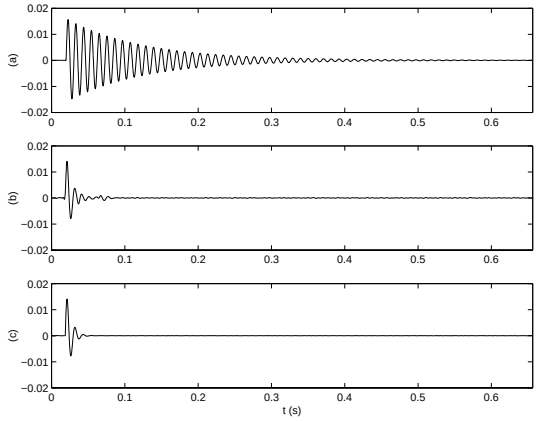

Fig. 12. Velocity response $\dot{x}$ (ms^{-1}) of the LQR impedance controlled system to a step disturbance current I_1. (a) experimental open-loop, (b) closed-loop (b), and (c) simulated closed-loop.

are met, i.e., the plant is minimal, proper, controllable, observable, and of finite dimension. However, in order to find a solution using existing tools, i.e., the algebraic Riccati solution implemented by the μ-Synthesis Toolbox for Matlab©, the system must meet some additional requirements. The most problematic of which, is the requisite full rank condition on the standard plant matrices D_{21} and D_{12}. In this case, where each of the signals w, u, y, and z are uni-dimensional, this condition requires that the feed-through term from w to y, and u to z, is non-zero. As the performance signal z already contains a direct weighting on the control signal V_z, the only condition not met is that on D_{21}. To overcome this problem, for the purpose of controller synthesis, we include an artificial feed-through term D_{21}. We now have two design parameters: k_u and D_{21}. These were chosen to be 0.1 and 1 respectively. In the authors expererience, both parameters tend to have a similar effect on the controller bandwidth and closed-loop performance. As either is decreased, the controller bandwidth and closed-loop damping increases.

Under the same test conditions as discussed in Section IV-C.1, the damping performance of the $\mathcal{H}_2$ controller, was measured to be $19.25\ dB$.

V. Conclusions

Electromagnetic transducers have been employed extensively in active vibration control systems as force actuators, velocity sensors, or both. Compared to other transducers such as piezoelectric materials and shape memory alloys, the large stroke, physical robustness, high bandwidth, and low-cost render them useful in a wide range of applications.

In this paper, we have demonstrated that the connection of an electrical impedance to the terminals of an electromagnetic coil is equivalent to implementing a standard feedback controller around the mechanical system. By revealing the underlying feedback structure and casting it as a typical MIMO control problem, an impedance can be found that minimizes some arbitrary performance objective.

The presented techniques are successfully applied to the design and implementation of an LQR and $\mathcal{H}_2$ based, active impedance controller. Without the need for any external sensors, the resonant peak of an experimental single-degree-of freedom system was substantially reduced in magnitude by up to $19.4\ dB$.

VI. References

[1] E. H. Anderson, N. W. Hagood, and J. M. Goodliffe. Self-sensing piezoelectric actuation: Analysis and application to controlled structures. In *Proc. AIAA/ASME/ASCE/AHS/ASC Structures, Structural Dynamics, and Materials*, pages 2141–2155, 1992.

[2] C. Choi and K. Park. Self-sensing magnetic levitation using LC resonant circuits. *Sensors and Actuators*, pages 1276–1281, 1999.

[3] R. L. Clark and K. D. Frampton. Phase compensation for feedback control of enclosed sound fields. *Journal of Sound and Vibration*, 195(5):701–718, 1996.

[4] J. J. Dosch, D. J. Inman, and E. Garcia. A self-sensing piezoelectric actuator for collocated control. *Journal of Intelligent Material Systems and Structures*, 3:166–185, January 1992.

[5] A. Fleming and S. O. R. Moheimani. Improved current and charge amplifiers for driving piezoelectric loads, and issues in signal processing design for synthesis of shunt damping circuits. *Journal of Intelligent Material Systems and Structures*, Submitted August 2002.

[6] C. R. Fuller, S. J. Elliott, and P. A. Nelson. *Active Control of Vibration*. Academic Press, 1996.

[7] B. M. Hanson, M. D. Brown, and J. Fisher. Self sensing: Closed-loop estimation for a linear electromagnetic actuator. In *Proc. IEEE American Control Conference*, pages 1650–1655, Arlington, VA USA, June 2001.

[8] S. A. Lane and R. L. Clark. Improving loudspeaker performance for active noise control. *Journal of the Audio Engineering Society*, 46(6):508–519, June 1998.

[9] S. Mirzaei, S. M. Saghaiannejad, V. Tahani, and M. Moallem. Electromagnetic shock absorber. In *IEEE International Conference on Electric Machines and Drives Conference IEMDC 2001*, pages 760–764, 2001.

[10] N. Morse, R. Smith, B. Paden, and J. Antaki. Position sensed and self-sensing magnetic bearing configuations and associated robustness limitations. In *Proc. IEEE Conference on Decision and Control*, pages 2599–2604, Tampa, Florida USA, December 1998.

[11] S. S. Rao. *Mechanical Vibrations*. Addison-Wesley Publishing Company, 3rd edition, 1995.

[12] D. Vischer and H. Bleuler. Self-sensing active magnetic levitation. *IEEE Transactions on Magnetics*, 29(2):169–177, 1993.